

Modelling solid tumour growth using the theory of mixtures

HELEN BYRNE[†]

Division of Applied Mathematics, School of Mathematical Sciences, University of Nottingham, Nottingham NG7 2RD, UK

AND

LUIGI PREZIOSI[‡]

Dipartimento di Matematica, Politecnico di Torino, Corso Duca degli Abruzzi 24, 10129 Torino, Italy

[Received on 5 June 2001; revised on 7 June 2003; accepted on 5 July 2003]

In this paper the theory of mixtures is used to develop a two-phase model of an avascular tumour, which comprises a solid, cellular, phase and a liquid phase. Mass and momentum balances which are used to derive the governing equations are supplemented by constitutive laws that distinguish the two phases and enable the stresses within the tumour to be calculated. Novel features of the model include the dependence of the cell proliferation rate on the cellular stress and the incorporation of mass exchange between the two phases.

A combination of numerical and analytical techniques is used to investigate the sensitivity of equilibrium tumour configurations to changes in the model parameters. Variation of parameters such as the maximum cell proliferation rate and the rate of natural cell death yield results which are consistent with analyses performed on simpler tumour growth models and indicate that the two-phase formulation is a natural extension of the earlier models. New predictions relate to the impact of mechanical effects on the tumour's equilibrium size which decreases under increasing stress and/or external loading. In particular, as a parameter which measures the reduction in cell proliferation due to cell stress is increased a critical value is reached, above which the tumour is eliminated.

Keywords: cellular dynamics; tumour growth; deformable porous media.

1. Introduction

By the time that a cancer patient presents with clinical symptoms, it is likely that their primary tumour will measure several centimetres in diameter, be growing rapidly and have spread, or metastasized, to other parts of the patient's body. Such behaviour is characteristic of vascular tumours, that is those that have acquired a blood supply. The new vasculature provides them with an effectively limitless supply of oxygen and other nutrients that are needed to sustain rapid growth. The vasculature also provides a transport network to other parts of the body for small clusters of cells that break free from the primary tumour, enter the blood supply and may establish secondary tumours, or metastases, in other tissues.

Given that the event, or mutation, that initially triggered the tumour probably occurred several years earlier, it is natural to ask why the tumour was not detected sooner and

[†]Email: helen.byrne@nottingham.ac.uk

[‡]Email: preziosi@polito.it

why it suddenly started to grow rapidly. To resolve these issues we consider the different stages of cancer growth. Following a mutation which confers on a cell and its progeny an effective proliferative advantage (due, for example, to either an increase in the cell replication rate or a reduction in the rate of cell death), a cluster of cancerous cells forms which receives vital nutrients and oxygen from the surrounding normal tissue by diffusion. Initially all cells are well-nourished and proliferate rapidly. As the colony increases in size, cells towards the centre are progressively starved of oxygen and nutrients and, in consequence, their proliferation rate and the tumour's overall growth rate decline. If the oxygen concentration falls below a critical threshold value then the cells are unable to survive and undergo necrotic cell death. Eventually this avascular tumour will reach an equilibrium size (~ 2 mm in diameter, Folkman & Hochberg, 1973), at which the rates of cell proliferation and apoptosis, averaged over the tumour volume, balance. At this stage the tumour typically comprises an outer rim of proliferating cells, a central core of necrotic debris and an intermediate region of quiescent cells which are alive, but do not proliferate due to nutrient deprivation (Sutherland, 1988; Sutherland & Durand, 1984).

The switch from the slow and relatively harmless avascular growth phase described above to the rapid and life-threatening vascular growth phase occurs during a process termed angiogenesis (Carmeliet & Jain, 2000; Craft & Harris, 1994; Folkman, 1974). During angiogenesis, certain tumour cells, and quiescent cells in particular, secrete a range of diffusible proteins and chemicals that are known collectively as tumour angiogenic factors (TAFs). On reaching the neighbouring vasculature, the TAFs stimulate the endothelial cells that line the blood vessels to proliferate and sprout new capillary tips which migrate via chemotaxis and haptotaxis towards the tumour. Capillary tips that come into close proximity fuse together (or anastomose), forming closed loops, through which circulating blood may flow. Secondary sprouts emanate from the new loops and so the process continues, with increasing numbers of capillary tips being formed, until the new vessels penetrate the tumour and it commences vascular growth, as described above.

From a clinical perspective it is clearly of paramount importance to limit the growth and spread of vascular tumours and for this reason much current research is being directed towards developing effective strategies which limit or halt the development of the tumour's vasculature. Due to their spatio-temporal heterogeneity, it is difficult to perform reliable experiments involving vascular tumours. For this reason, considerable effort has been devoted to studying and manipulating the growth of avascular tumours *in vitro*. The majority of these experiments reinforce the roles played by nutrient and oxygen diffusion and consumption in sustaining the tumour's growth and development. More recently, mechanical effects have been shown to play an important role in tumour growth and development. For example, by culturing avascular tumours in gels of varying stiffness, Helmlinger *et al.* (1997) demonstrated that the resistance or stress exerted on tumour cells by their surroundings affects the tumour's equilibrium size, with stiffer gels giving rise to smaller tumours. Direct evidence that cell stress or pressure affects proliferation is provided by Curtis & Seehar (1971). When sheets of cells were mechanically deformed periodically, the cells' mitotic rates varied with the frequency of oscillation: low and high frequencies produced moderate rates of proliferation while intermediate levels produced the largest proliferation rates. In view of these results, it is natural to ask how the relative importance of these different mechanisms affects the growth of cells in general and solid tumours in

particular. Once these questions have been addressed it may be possible to design new treatments which improve the management of tumours.

From a mathematical viewpoint, the majority of models that describe the evolution of solid tumours are based on mass balance principles for cells and reaction diffusion equations for growth factors (see Byrne, 2003 for a recent review). The main challenges involved in developing such models are in describing how the tumour cells migrate, reproduce and die and how the various chemicals diffuse, are produced and taken up by the cells. In the earliest models (Adam, 1987; Greenspan, 1972; McElwain & Morris, 1978), attention focused on a single population of tumour cells. Their density was taken to be constant and the tumour's growth assumed to be one-dimensional. Under these assumptions a closed system of equations was obtained. Mathematical models of this type usually comprise a reaction–diffusion equation for the distribution, within the tumour, of chemicals of interest (e.g. oxygen, glucose or growth-inhibitory drugs) and an integro-differential equation characterizing the tumour's volumetric growth rate (Adam, 1987; Greenspan, 1972; McElwain & Morris, 1978). Such models have enjoyed considerable success, reproducing the multilayered spatial patterns that characterize the development of multicellular spheroids cultured *in vitro* (Kunz-Schughart *et al.*, 2000; Sutherland, 1988).

When interest in describing the development of three-dimensional tumours containing one or more cell populations arose, difficulties in closing the system of mass balance equations became apparent. To resolve these difficulties, Ward & King (1997, 1998, 1999) assumed that all cells moved with the same velocity and that the tumour was radially symmetric. When studying the stability of radially-symmetric tumours to asymmetric perturbations both Greenspan (1976) and Byrne & Chaplain (1997) invoked Darcy's law to close their model equations.

We remark that none of the mathematical models discussed thus far permit investigation of the impact that mechanical phenomena may have on the tumour's development. An alternative approach, which allows such investigations, involves deriving mass and momentum balance equations for each cell population. When developing the momentum balance equations, consideration of cell-to-cell mechanical interactions is required and constitutive laws must be employed to describe such interactions. This multiphase modelling approach, which has been widely used in industrial applied mathematics (Drew & Segel, 1971; Fowler, 1997) was first used to describe solid tumour growth by Please and co-workers (Landman & Please, 2001; Please *et al.*, 1998). More recently, Ambrosi & Preziosi (2002) have examined the implications of alternative ways of closing the mass and momentum balance equations. Two of the proposed closures provide a mechanical basis for using Darcy's law to relate the velocities of the different cell populations to their respective pressures. They are based on the assumption that the tumour cells either move on an extracellular matrix, sliding over the network as a viscous fluid, or that they seek less crowded regions, while maintaining contact with neighbouring cells.

In this paper, we use the modelling framework presented in Ambrosi & Preziosi (2002) to develop a mathematical description of an avascular tumour as a multiphase system or, more precisely, as a saturated porous material. The solid skeleton is composed of deformable balloons (the cells) and is bathed in an organic liquid containing diffusible nutrients and growth factors. For simplicity we assume that all tumour cells are of the same type, and view the solid skeleton as a homogeneous material.

While the use of multiphase models in biomechanics is not new, existing models have been developed mainly to study bones and cartilage (Barker & Seedhom, 1997; Hou *et al.*, 1989; Frijns *et al.*, 1997; Mow & Lai, 1979; Wu & Epstein, 1997), and, to a lesser extent, soft tissues, such as heart (Sorek & Sideman, 1986; Yang *et al.*, 1994), lungs (Lai-Fook, 1988), and brain (Nicholson, 1985) (for additional references, see Preziosi, 1996). In these studies, growth is neglected and attention focuses on the flow of the extracellular fluid through the tissue, or solid, phase and its mechanical response to the flow. When modelling solid tumours, mass exchange between the solid and liquid phases is of fundamental importance. In addition to including this feature, our multiphase model enables us to determine the stress distribution inside the tumour, to describe mechanical interactions with the surrounding medium and to consider proliferation rates which depend on local cellular stress. The model also includes viscous effects in the motion of cells. In the one-dimensional case the model reduces to a mixed system of partial differential equations for the cell volume fraction, the cell velocity, the nutrient concentration and the size of the tumour. In the poroelastic limit (i.e. when viscous effects are neglected), the model equations further simplify to a pair of nonlinear parabolic equations for the cell volume fraction and the nutrient concentration.

The simulations that we perform focus on the existence of time-independent, equilibrium solutions and their dependence on the model parameters (by contrast, in Breward *et al.* (2002) attention focuses on the tumour's evolution, using a similar, two-phase model). We find that the tumour size increases as the maximum rate of cell proliferation, which is realized under nutrient-rich stress-free conditions, increases (or as the rate of natural cell death or apoptosis decreases). The simulations also indicate that when the growth coefficient and, therefore, the equilibrium tumour size increase above critical values a non-compact, necrotic region, containing few or no living tumour cells, forms at the centre of the tumour. These results are consistent with sensitivity analyses performed using other, simpler models (Adam, 1987; Greenspan, 1972; McElwain & Morris, 1978). The good qualitative agreement between the different models indicates that our model is a natural extension of the earlier models. In fact, in Byrne *et al.* (2003) it is shown how models that are similar to the earlier solid tumour growth models may be obtained from our multiphase model under suitable restrictive assumptions.

As already mentioned, one of the novel features of our multi-phase formulation is the ability to study the impact of stress-dependent cell proliferation and the external loading of the tumour. The equilibrium tumour size decreases under both increasing stress and external loading. In the former case there is a finite, critical value of the parameter which measures the inhibitory influence of cell stress on proliferation above which the tumour disappears. To understand the biological implications of these results, consider a tumour growing *in vivo*. As it expands, the tumour will compress the surrounding, normal tissue, which will, in turn, exert a stress or loading on the tumour. Our model suggests that, depending on the environmental conditions and the sensitivity of the cells to mechanical cues, such a tumour may evolve to a nutrient-limited equilibrium configuration or a stress-limited equilibrium solution. In order to investigate whether manipulation of mechanical effects is a promising direction for cancer therapy, new experiments must be designed in which avascular tumours are grown in stressed environments. This may be achieved by culturing the tumour cells in gels of varying stiffness (Helmlinger *et al.*, 1997), or within elastic membranes of known compliance.

The remainder of the paper is organized in the following way. In Section 2 we use the theory of mixtures to formulate a general two-phase model which we specialize in Section 3 to describe avascular tumour growth. The model is simplified in Section 4 where attention focuses on one-dimensional Cartesian growth. Novel features of our model, as compared with existing descriptions of avascular tumour growth (Adam, 1987; Greenspan, 1972; McElwain & Morris, 1978), include the dependence of the tumour cell proliferation rate on the cell pressure (or stress) and the exchange of material between the cell and water phases that accompanies cell proliferation and death. Using a combination of numerical and analytical techniques, the size and structure of the steady-state solutions of the one-dimensional model are investigated in Section 5, with particular attention paid to the way in which these solutions depend on key model parameters such as the rate at which the cells proliferate and undergo natural cell death and the sensitivity of the proliferation rate to the cellular pressure. The paper concludes in Section 6 with a summary and brief discussion of the key results.

2. The theory of mixtures applied to multicell spheroids

The starting point that we use to develop our model for multicell spheroids as deformable porous media is the theory of mixtures. This is a theory based on balance laws and conservation principles which is well known in continuum mechanics (Bowen, 1976, 1980; Farina & Preziosi, 2000; Rajagopal & Tao, 1995), and has been widely applied to systems which can be schematized as a mixture of interacting continua.

For simplicity, we assume that the tumour comprises two constituents only: a solid phase (the living tumour cells) and a liquid phase (the extracellular fluid in which the cells live). This means that we are considering the avascular phase of tumour growth and assuming that dead cells disintegrate instantaneously into waste products and re-usable materials (i.e. extracellular fluid). In addition, the motion of the cells and the intercellular fluid is so slow that inertial terms can be neglected and we can write

$$\rho_T \left[\frac{\partial \phi_T}{\partial t} + \nabla \cdot (\phi_T \mathbf{v}_T) \right] = \Gamma_T, \quad (2.1)$$

$$\rho_l \left[\frac{\partial \phi_l}{\partial t} + \nabla \cdot (\phi_l \mathbf{v}_l) \right] = -\Gamma_T, \quad (2.2)$$

$$\nabla \cdot \mathbb{T}_m = 0, \quad (2.3)$$

$$\nabla \cdot \mathbb{T}_T + m_T = 0 = \nabla \cdot \mathbb{T}_l + \mathbf{m}_l, \quad (2.4)$$

where the subscripts T and l denote, respectively, quantities associated with the cellular and liquid phases. In particular, ρ_p is the ‘true’ density, that is the density of the liquid and of the tumour cell, which are assumed constant (incompressibility of the constituents); ϕ_p is the volume fraction, i.e. the volume occupied by the p th-constituent over the total volume; \mathbf{v}_p is the velocity of the constituent; \mathbb{T}_T is the partial stress tensor relative to the cellular phase and \mathbb{T}_m is the stress tensor of the mixture as a whole; Γ_T is the mass supply absorbed by the liquid phase; and \mathbf{m}_l is the momentum supply related to the local, interfacial interactions between the constituents.

If the mixture is saturated, then the following geometrical constraint must also be added

to the model equations:

$$\sum_{p=1}^N \phi_p = 1. \quad (2.5)$$

As we discuss in the following section, this constraint leads naturally to an equation for the divergence of a velocity field and an indeterminacy in the constitutive equations for the stresses. As such, there is a clear analogy between the geometrical constraint (2.5) and the incompressibility assumption in fluid mechanics.

3. Deformable porous media model

Equations (2.1)–(2.4) are closed by introducing suitable constitutive relations for Γ_T , \mathbb{T}_m , \mathbb{T}_l , and \mathbf{m}_l . The choice of Γ_T may be determined from phenomenological observations of cell proliferation and death. Regarding the other terms, it is possible to show that the saturation assumption of the constituents implies the presence of a Lagrange multiplier (Farina & Preziosi, 2000; Rajagopal & Tao, 1995). In consequence, the constitutive equations may be characterized by a ‘pressure’ contribution and an excess part in the following manner:

$$\mathbb{T}_T = -\phi_T P \mathbb{I} + \tilde{\mathbb{T}}_T, \quad (3.1)$$

$$\mathbb{T}_m = -P \mathbb{I} + \tilde{\mathbb{T}}_m, \quad (3.2)$$

$$\mathbf{m}_l = P \nabla \phi_T + \tilde{\mathbf{m}}_T. \quad (3.3)$$

Equation (3.2) implies that the momentum equation for the mixture (2.3) can be rewritten as

$$\nabla P = \nabla \cdot \tilde{\mathbb{T}}_m, \quad (3.4)$$

We now focus on the constitutive equation for the stress tensor \mathbb{T}_T supposing that the assumption of constituent separation holds (Ambrosi & Preziosi, 2002; Ehlers, 1993; Farina & Preziosi, 2000): that is, each free energy depends on quantities related to its constituents only. More specifically, it is known that cells are linked to each other by receptors which give rise to strong, short-range cell–cell interactions. Therefore, the state of stress will depend not only on the state of deformation, but also on how quickly the deformation occurs. We will assume that the solid-phase free energy (and hence \mathbb{T}_T) depends on ϕ_T , \mathbb{F}_T , $\dot{\mathbb{F}}_T$, and $\mathbf{v}_l - \mathbf{v}_T$ where \mathbb{F}_T is the deformation gradient relative to the cellular phase.

Now, the state of stress of a multicell spheroid does not change if it undergoes a deformation which is locally volume preserving. This means, for instance, that if two cells switch places they will tend not to return to their original positions. Additionally, the stress that a cell experiences will be the same as that felt by the other cell when it occupied the same position. Under this assumption we deduce that, for all unimodular transformations \mathbb{H} ,

$$\mathbb{T}_T(\mathbb{F}_T, \dot{\mathbb{F}}_T) = \mathbb{T}_T(\mathbb{F}_T \mathbb{H}, \dot{\mathbb{F}}_T \mathbb{H}). \quad (3.5)$$

In particular, this must be true for the unimodular transformation

$$\mathbb{H} = (\det \mathbb{F}_T) \mathbb{F}_T^{-1}, \quad (3.6)$$

and, therefore,

$$\mathbb{T}_T(\mathbb{F}) = \mathbb{T}_T(\det \mathbb{F}_T, \det \mathbb{F}_T \dot{\mathbb{F}}_T \mathbb{F}_T^{-1}) = \widehat{\mathbb{T}}_T(\phi_T, \nabla \mathbf{v}_T), \quad (3.7)$$

as

$$\det \mathbb{F}_T = \phi_* / \phi_T \quad \text{and} \quad \dot{\mathbb{F}}_T \mathbb{F}_T^{-1} = \nabla \mathbf{v}_T, \quad (3.8)$$

where ϕ_* is the natural volume ratio corresponding to a vanishing state of stress. Objectivity requires that $\widehat{\mathbb{T}}_T$ depend on the velocity gradient via its symmetric part \mathbb{D}_T and, further, that $\widehat{\mathbb{T}}_T$ is an isotropic function of \mathbb{D}_T .

Appealing to Wang's representation theorem (Wang, 1969, 1970), we deduce that

$$\widehat{\mathbb{T}}_T(\phi_T, \mathbb{D}_T) = -\Sigma \mathbb{I} + k_1 \mathbb{D}_T + k_2 \mathbb{D}_T^2, \quad (3.9)$$

where Σ , k_1 and k_2 are functions of ϕ_T and the principal invariants of \mathbb{D}_T . Assuming that cell and fluid velocities are very slow, that they are analytic in the principal invariants and that the components of \mathbb{D}_T are first-order quantities, we can linearize (3.9) to obtain

$$\widehat{\mathbb{T}}_T(\phi_T, \mathbb{D}_T) = (-\Sigma + \lambda_T \nabla \cdot \mathbf{v}_T) \mathbb{I} + 2\mu_T \mathbb{D}_T, \quad (3.10)$$

where Σ , λ_T and μ_T may be functions of the volume ratio ϕ_T . In conclusion, the constitutive equation for \mathbb{T}_T resembles that of a viscous compressible fluid. It must be stressed that, in practice, neither λ_T nor μ_T will be constant as viscous forces between cells increase, at least linearly, with their volume ratio.

Due to the phase separation hypothesis, we can assume

$$\mathbb{T}_l = -\phi_l P \mathbb{I}. \quad (3.11)$$

Focusing on the interfacial forces, but without going into thermodynamical details, we note that if the interfacial forces are assumed to depend (at most linearly) on the growth terms and on the relative velocity $\mathbf{v}_T - \mathbf{v}_l$ which is frame invariant, then

$$\mathbf{m}_T = P \nabla \phi_T + \Lambda_T (\mathbf{v}_l - \mathbf{v}_T) + \alpha_T \Gamma_l (\mathbf{v}_l - \mathbf{v}_T) + \beta_T \Gamma_T (\mathbf{v}_l - \mathbf{v}_T), \quad (3.12)$$

$$\mathbf{m}_l = P \nabla \phi_l + \Lambda_l (\mathbf{v}_l - \mathbf{v}_T) + \alpha_l \Gamma_l (\mathbf{v}_l - \mathbf{v}_T) + \beta_l \Gamma_T (\mathbf{v}_l - \mathbf{v}_T). \quad (3.13)$$

In (3.12) and (3.13) $\Lambda_j, \alpha_j, \beta_j$ ($j = T, l$) are constants which we determine below. When considering \mathbf{m}_T and \mathbf{m}_l , it should not be necessary to mention whether we are focusing on the liquid or the cell phase: switching the indices should yield the same relation. This symmetry condition gives the following relations:

$$\Lambda_l = -\Lambda_T \quad \beta_l = -\alpha_T, \quad \beta_T = -\alpha_l. \quad (3.14)$$

Therefore

$$\mathbf{m}_T + \mathbf{m}_l = (\alpha_T + \alpha_l) (\Gamma_l - \Gamma_T) (\mathbf{v}_l - \mathbf{v}_T), \quad (3.15)$$

which, recalling (2.4), satisfies (2.3) only if $\alpha_T + \alpha_l = -1/2$. This allows us to write (3.12) and (3.13) as

$$\mathbf{m}_T = P\nabla\phi_T + \Lambda_T(\mathbf{v}_l - \mathbf{v}_T) + \frac{\Gamma_T}{2}(\mathbf{v}_l - \mathbf{v}_T), \quad (3.16)$$

$$\mathbf{m}_l = P\nabla\phi_l + \Lambda_T(\mathbf{v}_T - \mathbf{v}_l) + \frac{\Gamma_l}{2}(\mathbf{v}_T - \mathbf{v}_l), \quad (3.17)$$

or

$$\mathbf{m}_T = P\nabla\phi_T + \left(\Lambda_T + \frac{\Gamma_T}{2}\right)(\mathbf{v}_l - \mathbf{v}_T), \quad (3.18)$$

$$\mathbf{m}_l = P\nabla\phi_l - \left(\Lambda_T - \frac{\Gamma_T}{2}\right)(\mathbf{v}_l - \mathbf{v}_T). \quad (3.19)$$

Referring to Farina & Preziosi (2001) it is possible to verify that (3.12) and (3.13) are compatible with the second law of thermodynamics. Indeed, in Farina & Preziosi (2001) the same relation is derived on the basis of thermodynamics.

Substituting with (3.11) and (3.19) in (2.4), the momentum equation for the liquid becomes

$$-\phi_l\nabla P + \left(\Lambda_T - \frac{\Gamma_T}{2}\right)(\mathbf{v}_l - \mathbf{v}_T) = 0. \quad (3.20)$$

If $\Gamma_T = 0$ and the permeability coefficient is defined as $K = \mu\phi_l^2/\Lambda_T$, (3.20) gives rise to the usual form of Darcy's law for a deformable porous material:

$$\phi_l(\mathbf{v}_l - \mathbf{v}_T) = -\frac{K}{\mu}\nabla P. \quad (3.21)$$

Using the definition of permeability K introduced above, we note that in the general case (when $\Gamma_T \neq 0$), a correction term appears in Darcy's law:

$$\phi_l(\mathbf{v}_l - \mathbf{v}_T) = -\frac{K}{\mu(1-\gamma)}\nabla P, \quad (3.22)$$

where

$$\gamma = \frac{K\Gamma_T}{2\mu\phi_l^2}. \quad (3.23)$$

Thus Darcy's law emerges from our model, even in the general case. Consequently, we conclude that the assumptions used to develop our two-phase model provide a possible description of behaviour at a more fundamental level that is needed to obtain Darcy's law. Moreover, that Darcy's law emerges naturally from our modelling framework provides further justification for its use to describe fluid flow through porous solids.

We anticipate that, for biological problems, the dimensionless coefficient γ will be extremely small: that is, momentum transfer associated with phase change will be negligible compared to that caused by drag. Therefore, its contribution to the

permeability coefficient will be masked by experimental errors associated with measuring the permeability coefficient and we may write $\hat{K} = K(\phi_T)/\mu$.

Equation (3.22) enables us to write \mathbf{v}_l in terms of the other variables:

$$\mathbf{v}_l = \mathbf{v}_T - \frac{\hat{K}}{1 - \phi_T} \nabla P. \quad (3.24)$$

By taking suitable combinations of (2.1) and (2.2) and using (3.26) to eliminate \mathbf{v}_l we obtain

$$\nabla \cdot (\mathbf{v}_T - \hat{K} \nabla P) = \left(\frac{1}{\rho_T} - \frac{1}{\rho_l} \right) \Gamma_T. \quad (3.25)$$

Finally, we must consider the evolution of the nutrient. Since the nutrient molecules are diffusing in a moving fluid and being absorbed by the tumour cells, we assume that their evolution is governed by the following advection–diffusion equation:

$$\frac{\partial n}{\partial t} + \nabla \cdot (n\mathbf{v}_l) = \nabla \cdot (k_n \nabla n) - \delta_n \phi_T n. \quad (3.26)$$

Summarizing, our model for a multicell spheroid as a deformable porous medium can be written as follows:

$$\left. \begin{aligned} \frac{\partial \phi_T}{\partial t} + \nabla \cdot (\phi_T \mathbf{v}_T) &= \frac{\Gamma_T}{\rho_T} \\ \nabla \cdot (\mathbf{v}_T - \hat{K} \nabla P) &= \left(\frac{1}{\rho_T} - \frac{1}{\rho_l} \right) \Gamma_T \\ \nabla P &= -\Sigma' \nabla \phi_T + \nabla (\lambda_T \nabla \cdot \mathbf{v}_T) + \nabla \cdot [\mu_T (\nabla \mathbf{v}_T + (\nabla \mathbf{v}_T)^T)] \\ \frac{\partial n}{\partial t} + \nabla \cdot \left(n\mathbf{v}_T - \frac{n\hat{K}}{1 - \phi_T} \nabla P \right) &= \nabla \cdot (k_n \nabla n) - \delta_n \phi_T n. \end{aligned} \right\} \quad (3.27)$$

In (3.27) the state variables are ϕ_T , \mathbf{v}_T , P , and n and the function Σ is positive in compression, so that $\Sigma' = d\Sigma/d\phi_T > 0$.

The growth problem is a free-boundary problem with a material interface fixed on the tumour cells. This interface moves with velocity \mathbf{v}_T and

$$\mathbf{n} \cdot \frac{d\mathbf{x}_T}{dt} = \mathbf{n} \cdot \mathbf{v}_T. \quad (3.28)$$

It is important to note that the boundary conditions used to close equations (3.27) usually involve prescribing the external stress that acts on the solid and the pressure of the extracellular liquid. In the inviscid case this yields

$$P = P_{\text{ext}}, \quad \Sigma(\phi_T) = \Sigma_{\text{ext}} \implies \phi_T = \Sigma^{-1}(\Sigma_{\text{ext}}). \quad (3.29)$$

In the case of a stress-free boundary, we may impose

$$P = 0, \quad \Sigma(\phi_T) = 0 \implies \phi_T = \Sigma^{-1}(0), \quad (3.30)$$

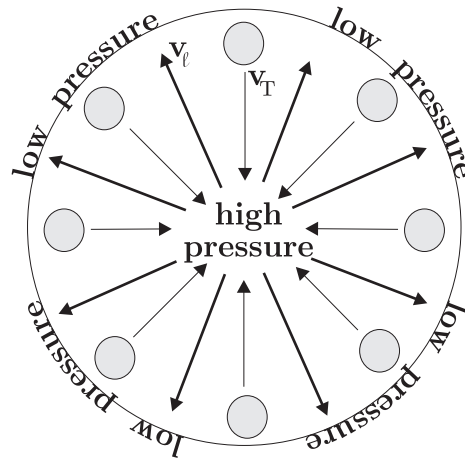


FIG. 1. Schematic diagram showing cell motion (thinner arrows) and extracellular fluid flow (thicker arrows) within a spherically symmetric avascular tumour.

where $\Sigma^{-1}(0)$ is called the natural volume ratio. In addition, Dirichlet boundary conditions are imposed on the nutrient equation

$$n = n_{\text{ext}}, \quad (3.31)$$

and initial distributions for ϕ_T and n are prescribed, together with the initial size of the tumour.

4. The one-dimensional case

In the one-dimensional case, if the tumour cell and liquid mass densities are equal then the model equations can be simplified. For example, adding equations (2.1) and (2.2) supplies

$$\frac{\partial}{\partial x}(\phi_T v_T + \phi_l v_l) = 0, \quad (4.1)$$

and can be integrated to give

$$\phi_T v_T + \phi_l v_l = \text{constant}. \quad (4.2)$$

By symmetry, both the liquid and cell velocities vanish at the tumour centre, so the integration constant is zero and

$$v_l = -\frac{\phi_T}{\phi_l} v_T. \quad (4.3)$$

Substituting with (4.3) in (3.24), we get

$$v_T = \hat{K} \frac{\partial P}{\partial x} \quad \text{and} \quad v_l = -\frac{\hat{K}(\phi_T)\phi_T}{1-\phi_T} \frac{\partial P}{\partial x}. \quad (4.4)$$

From a physical viewpoint, as the permeability \hat{K} is always positive, (4.4) imply that v_l is directed against the pressure gradient and v_T along it. As the pressure is higher inside the tumour than at its outer boundary, cells move towards the centre of the tumour and the extracellular liquid flows towards the boundary (see Fig. 1). A recirculation flow then forms: tumour cells near the centre die due to nutrient deprivation and generate re-usable, extracellular fluid. This liquid flows to the boundary where it is taken up by proliferating cells.

Using (4.4) we can eliminate the pressure from the model equations and rewrite them as

$$\left. \begin{aligned} \frac{\partial \phi_T}{\partial t} + \frac{\partial}{\partial x}(\phi v_T) &= \frac{\Gamma_T}{\rho_T} \\ \frac{\partial}{\partial x} \left[(\lambda_T + 2\mu_T) \frac{\partial v_T}{\partial x} \right] - \frac{v_T}{\hat{K}} - \Sigma' \frac{\partial \phi_T}{\partial x} &= 0 \\ \frac{\partial n}{\partial t} - \frac{\partial}{\partial x} \left(\frac{n \phi_T v_T}{1 - \phi_T} \right) &= k_n \frac{\partial^2 n}{\partial x^2} - \delta_n \phi_T n \end{aligned} \right\} \quad (4.5)$$

where k_n is assumed constant.

An interesting simplification occurs when viscous contributions are neglected. In this case, which corresponds to a classical poroelastic model, from (3.27) we have

$$\frac{\partial P}{\partial x} = -\frac{\partial \Sigma}{\partial x},$$

or $P + \Sigma = \text{constant}$. Using (4.4) we can then write

$$v_T = -\hat{K} \Sigma' \frac{\partial \phi_T}{\partial x}. \quad (4.6)$$

and eliminate v_T from the model equations to obtain

$$\frac{\partial \phi_T}{\partial t} = \frac{\partial}{\partial x} \left(\hat{K} \Sigma' \phi_T \frac{\partial \phi_T}{\partial x} \right) + \frac{\Gamma_T}{\rho_T}, \quad (4.7)$$

$$\frac{\partial n}{\partial t} + \frac{\partial}{\partial x} \left(\frac{\hat{K} \Sigma' \phi_T}{1 - \phi_T} \frac{\partial \phi_T}{\partial x} n \right) = k_n \frac{\partial^2 n}{\partial x^2} - \delta_n \phi_T n. \quad (4.8)$$

It should be noted that (4.8) is a nonlinear, parabolic equation, with a source term. Similar parabolic models have been proposed by other authors to describe tumour invasion (Gatenby & Gawlinski, 1996; Sherratt & Nowak, 1992). In these models the ‘cell diffusion’ term describes random motion of the cells. By contrast, in our model drag and cell–cell interactions govern cellular diffusion.

In (4.8), the permeability coefficient $\hat{K} = K/\mu$ is non-negative, vanishes at $\phi_T = 1$, and the following, commonly used dependence on ϕ_T will be assumed:

$$\hat{K}(\phi_T) = \frac{K_0}{\mu} (1 - \phi_T)^\kappa. \quad (4.9)$$

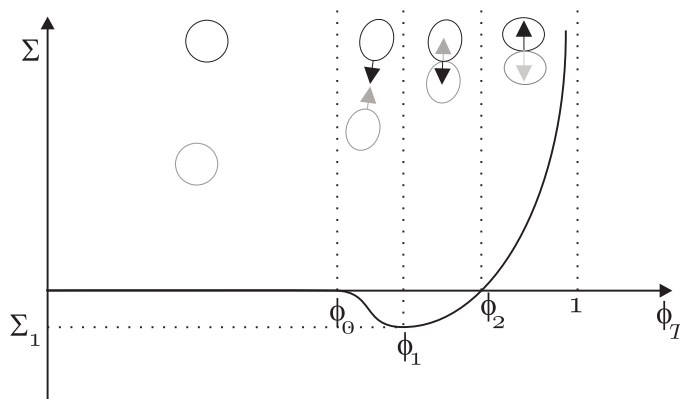


FIG. 2. Schematic diagram showing how the function $\Sigma(\phi_T)$ varies with ϕ_T . The black arrows represent the forces experienced by the black cells due to the presence of the grey cells (and conversely).

Less straightforward is the choice of $\Sigma(\phi_T)$. Whilst cells may experience compression and traction, they will only experience these forces if they are close enough to each other. To be more specific, we consider the following phenomenological description:

- Two cells which are far apart ignore each other;
- If the distance between two cells falls below a threshold value then they attract each other;
- When cells in contact are pulled apart, an adhesive force competes with cell separation;
- If two cells are too close together, they experience a repulsive force;
- The repulsive force becomes infinite in the limit as the cells are packed so densely that they fill the whole control volume.

In the one-dimensional case, let L represent the size of a ‘square’ cell and x the distance between adjacent cells. Then $\phi_T = L/(L + x)$ and the previous description can be reformulated as follows:

- Cell in regions where $\phi_T < \phi_0$ experience neither attractive nor repulsive forces;
- The attractive force attains a maximum value ($\Sigma = \Sigma_1$) when $\phi_T = \phi_1 > \phi_0$;
- The attractive and repulsive forces balance when $\phi_T = \phi_2 > \phi_1$
- The repulsive force becomes infinite as ϕ_T tends to one.

A function $\Sigma(\phi_T)$ that satisfies the above hypotheses is

$$\Sigma = \begin{cases} \alpha \frac{(\phi_T - \phi_0)^2 (\phi_T - \phi_2)}{(1 - \phi_T)^\beta} & \text{if } \phi_T > \phi_0; \\ 0 & \text{otherwise.} \end{cases} \quad (4.10)$$

In (4.10)

$$\beta = \frac{(1 - \phi_1)(3\phi_1 - 2\phi_2 - \phi_0)}{(\phi_1 - \phi_0)(\phi_2 - \phi_1)}, \quad (4.11)$$

and

$$\alpha = \frac{-\Sigma_1(1 - \phi_1)^\beta}{(\phi_1 - \phi_0)^2(\phi_2 - \phi_1)}. \quad (4.12)$$

With Σ defined by (4.10), equation (4.8) is a degenerate parabolic equation if $\phi_T > \phi_1$. It becomes a backward heat equation if $\phi_T < \phi_1$ and a hyperbolic equation if $\phi_T < \phi_0$. Referring to Fig. 2 this means that for any compressive force there is a unique equilibrium state. For moderate tensile stresses, there are two equilibria: an unstable state with $\phi_T < \phi_1$ and a stable state with $\phi_T > \phi_1$. For larger tensile stress there is no equilibrium configuration (this would correspond to rupturing the multicellular spheroid). Plotting the equilibrium states against the applied force (considered as a bifurcation parameter) there is a turning point at $\Sigma = \Sigma_1$ with a stable branch above $\phi_T = \phi_1$ and an unstable branch below it.

The dynamics will then avoid the volume ratios corresponding to the backward heat equations which is known to be characterized by short wave instability (or Hadamard instability; Bellomo & Preziosi, 1995). In fact, if, for instance, ϕ_T is increasing in a certain interval, then Σ is decreasing and the pressure increasing. From (4.4) this implies that $v_T > 0$ and, hence, that more tumour cells will move into the region, steepening $\frac{\partial \phi_T}{\partial x}$. This situation persists until $\phi_T > \phi_1$.

More generally, to appreciate why in practice our model does not become ill-posed, consider the equation $\frac{\partial u}{\partial t} = \frac{\partial}{\partial x}(k(u)\frac{\partial u}{\partial x})$ with $k(u)$ negative in a certain interval, $u \in [a, b]$ say, and positive elsewhere. Depending on the boundary conditions, of course, if the solution is such that $u < b$ within the spatial domain, a shock will form, across which u jumps between the extremal values a and b . In particular, u will form a shock rather than attaining values for which the equation is ill-posed (Elliott, 1985; Witelski, 1995).

For the sake of completeness, cells in regions where $\phi_T < \phi_0$ have no mechanical interactions with other cells ($\Sigma = 0$) and float freely. If the nutrient level in this region is such that $\Gamma_T < 0$ then, from (4.8), this situation persists and ϕ_T tends to zero. In the following we refer to this region as a ‘non-compact necrotic core’.

The growth term Γ_T is constructed on the basis of the following phenomenological observations:

- Proliferation occurs if the nutrient concentration exceeds the threshold value \bar{n} . Where $n (> \bar{n})$ is close to \bar{n} the proliferation rate is proportional to $n - \bar{n}$; as n increases, the proliferation rate eventually saturates.
- Cell proliferation is strongly affected by the presence of other cells which exert stress on the membrane of the replicating cell. In particular, the proliferation rate approaches zero as the volume ratio approaches one.
- Apoptosis is proportional to the volume ratio of cells.
- Necrosis occurs if the nutrient concentration falls below the threshold value \bar{n} and increases as n decreases.

A suitable function Γ_T , which combines these features and is continuous across $n = \bar{n}$, is

given by

$$\frac{\Gamma_T}{\rho_T} = \begin{cases} \frac{\gamma\phi_T}{1 + \sigma\Sigma(\phi_T)} \frac{n - \bar{n}}{1 + \nu n} - \delta\phi_T & \text{if } n > \bar{n}; \\ -\frac{1 + \mu\bar{n}}{1 + \mu n} \delta\phi_T & \text{otherwise.} \end{cases} \quad (4.13)$$

In (4.13), $\gamma, \sigma, \bar{n}, \delta$ and μ are positive constants. In more detail, the first term in (4.13) represents the rate of cell proliferation, the second the rate of apoptosis and the third the rate of necrosis.

Non-dimensionalization

It is convenient to reformulate the model equations in terms of the following dimensionless variables:

$$\tilde{t} = \delta_n t, \quad \tilde{x} = \sqrt{\frac{\delta_n}{k_n}} x, \quad \tilde{n} = \frac{n}{n_{\text{ext}}}, \quad \tilde{\phi}_T = \phi_T.$$

Thus we rescale time with the nutrient consumption timescale, distance with the nutrient diffusion lengthscale and the nutrient concentration with its value of the tumour boundary (note that the cellular volume fraction ϕ_T is already dimensionless). Under these rescalings the initial boundary value problem can be rewritten as

$$\frac{\partial \phi_T}{\partial \tilde{t}} = \tilde{D} \frac{\partial}{\partial \tilde{x}} \left(\tilde{K}(\phi_T) \tilde{\Sigma}'(\phi_T) \phi_T \frac{\partial \phi_T}{\partial \tilde{x}} \right) + \hat{\Gamma}_T \phi_T, \quad (4.14)$$

$$\frac{\partial \tilde{n}}{\partial \tilde{t}} + \tilde{D} \frac{\partial}{\partial \tilde{x}} \left(\frac{\tilde{K}(\phi_T) \tilde{\Sigma}'(\phi_T) \phi_T}{1 - \phi_T} \frac{\partial \phi_T}{\partial \tilde{x}} \tilde{n} \right) = \frac{\partial^2 \tilde{n}}{\partial \tilde{x}^2} - \phi_T \tilde{n}, \quad (4.15)$$

with

$$\frac{d\tilde{x}_T}{d\tilde{t}} = \tilde{K}(\phi_T) \tilde{\Sigma}'(\phi_T) \frac{\partial \phi_T}{\partial \tilde{x}} \quad \text{on } \tilde{x} = \pm \tilde{x}_T(\tilde{t}), \quad (4.16)$$

$$\phi_T = \phi_{\text{ext}}, \quad \tilde{n} = 1 \quad \text{on } \tilde{x} = \pm \tilde{x}_T(\tilde{t}). \quad (4.17)$$

In (4.14)–(4.17),

$$\tilde{K}(\phi_T) = (1 - \phi_T)^\kappa, \quad \tilde{\Sigma}(\phi_T) = \frac{1}{\alpha} \Sigma(\phi_T), \quad (4.18)$$

$$\hat{\Gamma}_T = \begin{cases} \frac{\tilde{\gamma}}{1 + \tilde{\sigma} \tilde{\Sigma}(\phi_T)} \frac{\tilde{n} - \hat{n}}{1 + \tilde{\nu} \tilde{n}} - \tilde{\delta} & \text{if } \tilde{n} > \hat{n}; \\ -\frac{1 + \tilde{\mu} \hat{n}}{1 + \tilde{\mu} \tilde{n}} \tilde{\delta} & \text{otherwise;} \end{cases} \quad (4.19)$$

and

$$\tilde{D} = \frac{K_0 \alpha}{\mu k_n}, \quad \tilde{\gamma} = \frac{\gamma n_{\text{ext}}}{\delta_n}, \quad \tilde{\delta} = \frac{\delta}{\delta_n}, \quad \tilde{\sigma} = \sigma \alpha, \quad \hat{n} = \frac{\bar{n}}{n_{\text{ext}}}, \quad \tilde{\mu} = \mu n_{\text{ext}}, \quad \tilde{\nu} = \nu n_{\text{ext}}. \quad (4.20)$$

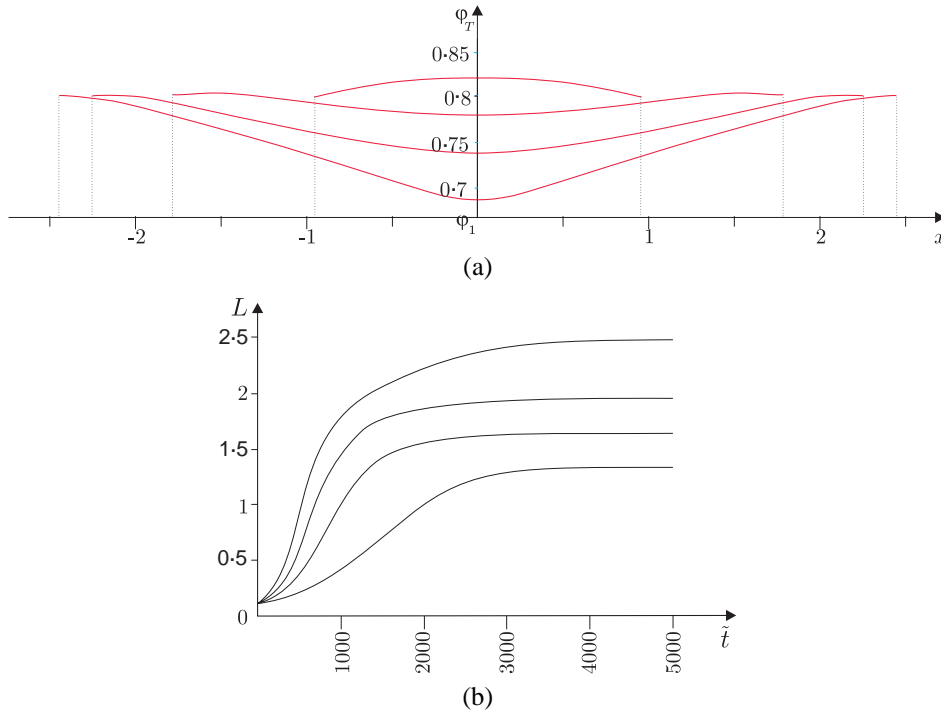


FIG. 3. (a) Diagram showing the evolution of the cell volume fraction $\phi_T(x, t)$ toward a steady state when $\tilde{\gamma} = 0.0125$, $\tilde{\delta} = 0.001$, and $\tilde{\sigma} = 0$ at times $t = 500, 1000, 2000, 4000$; (b) Diagram showing the evolution of the tumour width, $L(t)$, to its equilibrium value for different choices of $\tilde{\gamma}$. From the lower to the upper curve $\tilde{\gamma} = 0.005, 0.0075, 0.01, 0.0125$, while $\tilde{\delta} = 0.001$ and $\tilde{\sigma} = 0$.

It should be noted that in practice $\tilde{\gamma}, \tilde{\delta} \ll \tilde{D} \ll 1$. Therefore in (4.15) diffusion dominates convection as a transport mechanism. On the other hand, in (4.14) cell duplication/apoptosis is a much slower process than cell motion. Keeping this in mind, in the simulations that follow, we fix

$$\begin{cases} \tilde{D} = 0.1, & \kappa = 0.1, & \hat{n} = 0.5, & \tilde{\mu} = \tilde{\nu} = 0, \\ \phi_0 = 1/3, & \phi_1 = 2/3, & \phi_2 = 0.8, \end{cases} \quad (4.21)$$

($\phi_2 = 0.8$ has been measured by Netti *et al.* (1997)) and focus attention on how the solution profiles depend on other model parameters, such as $\tilde{\gamma}, \tilde{\delta}$ and $\tilde{\sigma}$.

Henceforth we omit the tildes from the independent and dependent variables, assuming, unless otherwise stated, that all variables are dimensionless.

Figure 3(a) shows how the tumour evolves towards a steady state in the stress-free case when the following parameter values are employed: $\tilde{\gamma} = 0.0125$, $\tilde{\delta} = 0.001$, and $\tilde{\sigma} = 0$. For this choice of parameters, at equilibrium the nutrient concentration at the tumour centre only just exceeds that which triggers central necrosis. In Fig. 3(a), a tumour of size $L = 0.1$ and constant density ϕ_2 is implanted at $t = 0$. We observe that at $t = 500$ the tumour is still so small that all cells have sufficient nutrient to replicate (i.e. $n > n_0$

everywhere). Further, the maximum cell compaction occurs at the tumour centre and, due to the repulsive forces they experience, cells move toward the tumour border, causing it to increase in size. At $t = 1000$ the nutrient concentration near the centre of the tumour falls below n_0 and cells there start to die. The location of the maximum cell volume fraction moves toward the tumour boundary, while in the centre a (local) minimum appears. Cells which are located in the central region of the tumour, between the two symmetric maxima, move toward the centre whereas those in the outer regions, between the maxima and the tumour boundary, move toward the boundary. Of course, the tumour still grows, but at a reduced rate (note the magnitude of the derivative of ϕ_T at the border). At $t = 4000$ the tumour has nearly reached its stationary configuration (presented in Fig. 4, lowest curve), at which the maximum cell volume fraction occurs on the tumour boundary. Figure 3(b) shows the temporal evolution of the tumour size for different values of $\tilde{\gamma}$. From the results we deduce that the equilibrium tumour size increases as the maximum cell proliferation rate $\tilde{\gamma}$ increases.

5. Stationary configurations

Preliminary analysis

The steady state is characterized by $\partial/\partial t = 0$ and a stationary tumour interface $x_T = L$, on which, from (4.16),

$$\frac{d\phi_T}{dx} = 0. \quad (5.1)$$

Since $\phi_T = \phi_{\text{ext}}$ on the boundary and the nutrient concentration decreases inside the domain, $\frac{d\phi_T}{dx} > 0$, $v_T < 0$ and $v_l > 0$ (see (4.3) and (4.7)). This means that, at equilibrium, there will be net movement of tumour cells toward the necrotic core which is balanced by a flux of extracellular liquid toward the tumour surface, the fluid being used to build new cells (see Fig. 1).

For simplicity, we fix the centre of the tumour at $x = 0$ and, in the following discussion, refer to positive values of x , for which $0 < x \leq L$. We assume in (4.19) that $\sigma = 0$ and that the model parameters are such that the non-compact region does not form. (The mechanisms by which the non-compact necrotic core forms and the case for which the growth rate depends on the cellular stress are discussed briefly at the end of this section.) In this case,

$$\hat{I}_T = \tilde{\gamma} \frac{(n - \hat{n})_+}{1 + \tilde{v}n} - \tilde{\delta} \in \left[-\tilde{\delta}, \frac{\tilde{\gamma}}{\tilde{v}} - \tilde{\delta} \right) \quad (5.2)$$

is an increasing function of n and has a unique zero at

$$n = n_0 \equiv \frac{\hat{n} + \frac{\tilde{\delta}}{\tilde{\gamma}}}{1 - \frac{\tilde{\delta}}{\tilde{\gamma}}\tilde{v}}. \quad (5.3)$$

Integrating the mass balance equation, it is possible to show that the steady state is characterized by the following balance between cell birth and death:

$$\int_0^L \hat{\Gamma}_T \phi_T \, dx = 0. \tag{5.4}$$

This means that a steady state will only be achieved if $n_0 < 1$, i.e. if

$$\hat{n} + (1 + \tilde{\nu}) \frac{\tilde{\delta}}{\tilde{\gamma}} < 1, \tag{5.5}$$

and if the tumour is large enough so that there are regions where n falls below the threshold value n_0 at which $\hat{\Gamma}_T = 0$. In particular, denoting by x_0 the value of x at which $n = n_0$, we deduce that for $x \in [x_0, L]$ the integral

$$\int_x^L \hat{\Gamma}_T \phi_T \, dy \tag{5.6}$$

is positive and has a maximum when $x = x_0$ and $n = n_0$.

Integrating (4.15) over the interval $[x_1, x_2]$, with $\partial/\partial t = 0$, one has

$$D(\phi_T(x_2)) \frac{d\phi_T}{dx}(x_2) - D(\phi_T(x_1)) \frac{d\phi_T}{dx}(x_1) = - \int_{x_1}^{x_2} \hat{\Gamma}_T \phi_T \, dy,$$

where

$$D(\phi_T) = \tilde{D} \tilde{K}(\phi_T) \tilde{\Sigma}'(\phi_T) \phi_T.$$

In particular,

$$D(\phi_T) \frac{d\phi_T}{dx} = \int_x^L \hat{\Gamma}_T \phi_T \, dy > 0,$$

and, therefore, ϕ_T is a monotonically increasing function of x , which (from the boundary conditions) attains a maximum at $x = L$ where $\phi_T(L) = \phi_{\text{ext}}$, or, in the stress-free case, $\phi_T(L) = \phi_2$.

Sensitivity analysis

We now focus on the sensitivity of the stationary solutions with respect to parameters associated with the cell proliferation rate, namely $\tilde{\gamma}$, $\tilde{\delta}$, and $\tilde{\sigma}$. All other parameters are held fixed at the values stated in (4.21). Apart from the last set of simulations, the boundary of the tumour is always assumed stress-free.

For the parameter values used in Fig. 4, inequality (5.5), which is a necessary condition for the existence of a stationary configuration, is satisfied if $\tilde{\gamma} > 2\tilde{\delta}$. If $0 < \tilde{\gamma}/(2\tilde{\delta}) - 1 \ll 1$, then the condition is barely satisfied, the size of the stationary tumour is very small, with $\phi_T \sim \phi_2 = 0.8$ for $|x| \leq L$, and the nutrient distribution is given by

$$n \approx \frac{\cosh \sqrt{\phi_2} x}{\cosh \sqrt{\phi_2} L}.$$

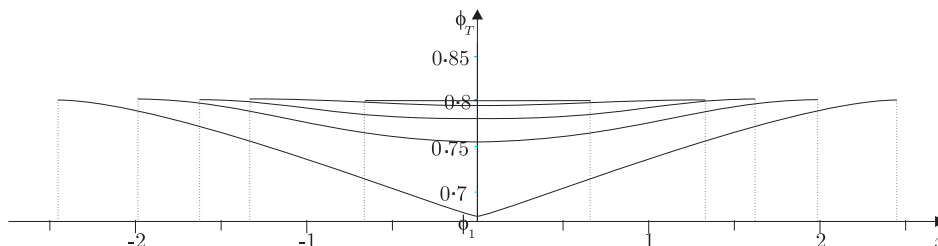


FIG. 4. Diagram showing the dependence of the steady-state cell distribution ϕ_T on $\tilde{\gamma}$. The vertical dotted lines mark the outer boundaries of the equilibrium tumours. As $\tilde{\gamma}$ increases the equilibrium tumour size increases and the cell volume fraction at the tumour centre decreases. Parameter values: $\tilde{\delta} = 0.001$, $\tilde{\sigma} = 0$, $\tilde{\gamma} = 0.0025, 0.005, 0.0075, 0.010, 0.0125$.

As the ratio $\tilde{\gamma}/\tilde{\delta}$ increases beyond 2, the tumour increases in size and the minimum value of ϕ_T , which occurs at $x = 0$, decreases. This situation pertains until a non-compact necrotic core is initiated at the tumour centre, i.e. until $\tilde{\gamma}/\tilde{\delta}$ passes through a threshold value at which $\phi_T(x = 0) = \phi_1$. This behaviour is depicted in Fig. 4 where we show how the tumour’s equilibrium size and cell distribution vary with $\tilde{\gamma}$ when $\tilde{\delta} = 0.001$ and $\tilde{\sigma} = 0$. In this case the non-compact necrotic core appears as $\tilde{\gamma}/\tilde{\delta}$ passes through a threshold value slightly above 0.0125.

We now assume that the parameter values are such that $\phi_T(x = 0) = \phi_1$, and a necrotic core is about to appear. Integrating the model equations for small x , and remembering that $dn/dx = 0$ at $x = 0$, in which case $n \sim n_1 + n_2x^2$ for some constants n_1 and n_2 , it is possible to show that near $x = 0$

$$\phi_T = \phi_1 + \Phi x,$$

with

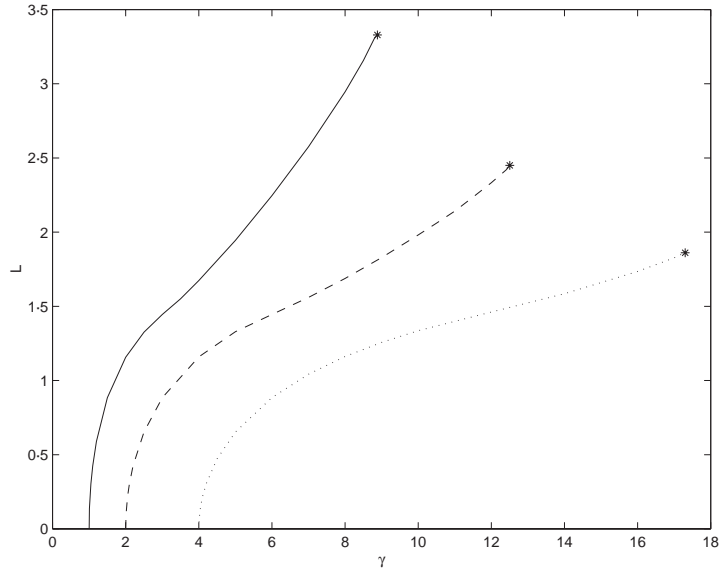
$$\Phi = \sqrt{-\frac{\hat{\Gamma}(n_1)\phi_1}{D'(\phi_1)}} = \sqrt{\frac{-\hat{\Gamma}(n_1)}{K(\phi_1)\Sigma''(\phi_1)}} = \sqrt{\frac{\delta}{K(\phi_1)\Sigma''(\phi_1)}}. \tag{5.7}$$

When $\tilde{\gamma}/\tilde{\delta}$ is very close to its threshold value ($\tilde{\gamma} = 0.0125$ and $\tilde{\delta} = 0.001$), the numerical simulations indicate that the slope of the ϕ_T curve approaches the value predicted in (5.7). In dimensionless terms this can be written as

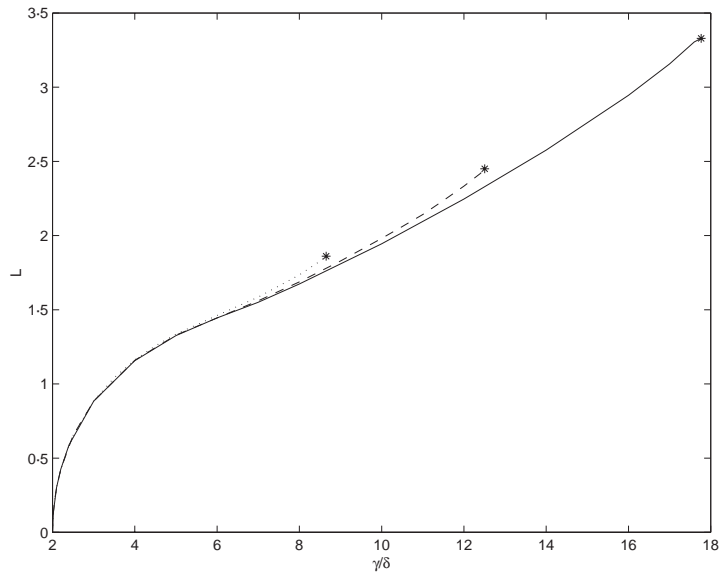
$$\phi_T = \phi_1 + 0.799\sqrt{\tilde{\delta}}x.$$

Referring to (4.6), we remark that, in this limit, $v_T(x = 0) = 0$ is automatically satisfied because $\Sigma'(\phi_T(x = 0)) = 0$. As a result, it is not necessary to impose $d\phi_T/dx(x = 0) = 0$.

The dependence of L on $\tilde{\gamma}$ is plotted in Fig. 5(a) for different values of $\tilde{\delta}$. The curves start at $\tilde{\gamma} = 2\tilde{\delta}$ with infinite slope and terminate, at the stars, when the non-compact region is initiated. By plotting in Fig. 5(b) L versus the ratio $\tilde{\gamma}/\tilde{\delta}$ we note that the three curves ‘merge’ to the same master curve for most values of $\tilde{\gamma}/\tilde{\delta}$, apart from values of $\tilde{\gamma}$ and $\tilde{\delta}$ near to which the necrotic core appears. Similar results are presented in Fig. 6 where we



(a)



(b)

FIG. 5. Series of sketches showing how the size of the equilibrium tumour L varies with $\tilde{\gamma}$ when $\tilde{\sigma} = 0$ and $\tilde{\delta} = 0.0005$ (solid line), $\tilde{\delta} = 0.001$ (dashed line), $\tilde{\delta} = 0.002$ (dotted line). (a) L against $\tilde{\gamma}$; (b) L against $\tilde{\gamma}/\tilde{\delta}$.

sketch L as $\tilde{\delta}$ varies for $\tilde{\gamma} = 2, 5, 10$. As in Fig. 5, the curves emanate from $\tilde{\delta} = \tilde{\gamma}/2$ with infinite slope and terminate at a critical point which coincides with the appearance of the non-compact necrotic core. The critical value of $\tilde{\gamma}$ at which this necrotic core is initiated

seems to increase with $\tilde{\delta}$ and the critical value of L seems to decrease with both $\tilde{\gamma}$ (Fig. 5) and $\tilde{\delta}$ (Fig. 6).

We now investigate the effect that making the cell growth rate depend on the cellular stress $\Sigma(\phi_T)$ has on the size and structure of the steady-state solutions. In (4.19) we take $\tilde{\sigma} \geq 0$. The results presented in Fig. 7 show that as $\tilde{\sigma}$ increases and, hence, the cell proliferation rate decreases more rapidly with increasing cellular stress, the equilibrium tumour becomes smaller and the cells more uniformly distributed across the tumour. In Fig. 8 we show how, for different values of the ratio $\tilde{\gamma}/\tilde{\delta}$, the equilibrium tumour size L decreases monotonically with $\tilde{\sigma}$. We emphasize once again that doubling $\tilde{\gamma}$ or halving $\tilde{\delta}$ yields the same result. The sketches indicate that if $\tilde{\sigma}$ is sufficiently large (e.g. $\tilde{\sigma} > 8.2$ when $\tilde{\gamma}/\tilde{\delta} = 10$) then no non-trivial equilibrium solutions exist and the tumour is eliminated. From a biological perspective, this suggests that it may be possible to control a tumour's size by making the cells more sensitive to mechanical compression, for example by making their mitotic or apoptotic rates depend on the stress.

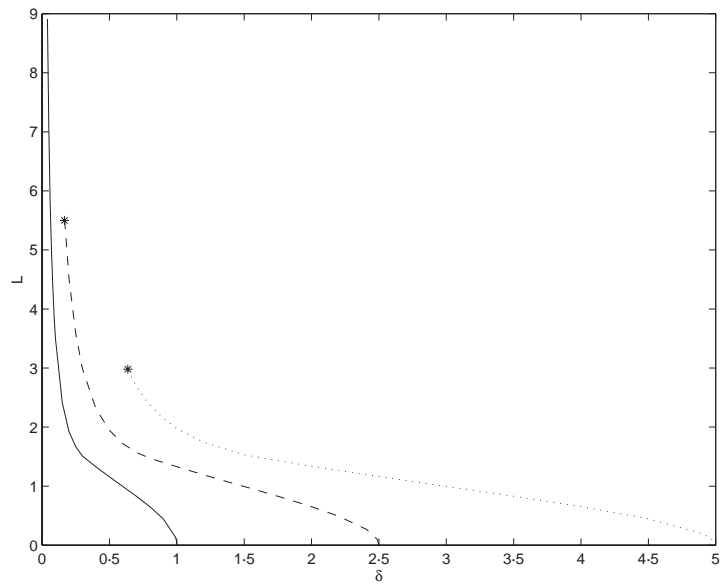
Figure 9 shows how the size of the tumour L decreases as the volume fraction on $x = L$ (or, equivalently, the applied load) increases. We remark that the reduction in L is less pronounced than that presented in Fig. 8.

Referring to Figs 8 and 9, we note that the external stress acting on a tumour which is growing in an organic tissue is caused by compression of the surrounding tissue, the ability of the tumour to degrade the tissue (through the secretion of proteases; Stetler-Stevenson *et al.*, 1993) and the ability of the external tissue to withstand stress and replace degraded cells. The results from our model indicate that tumour growth may be limited not only by the availability of nutrients but also by the stress exerted on the tumour by the tissue into which it is growing.

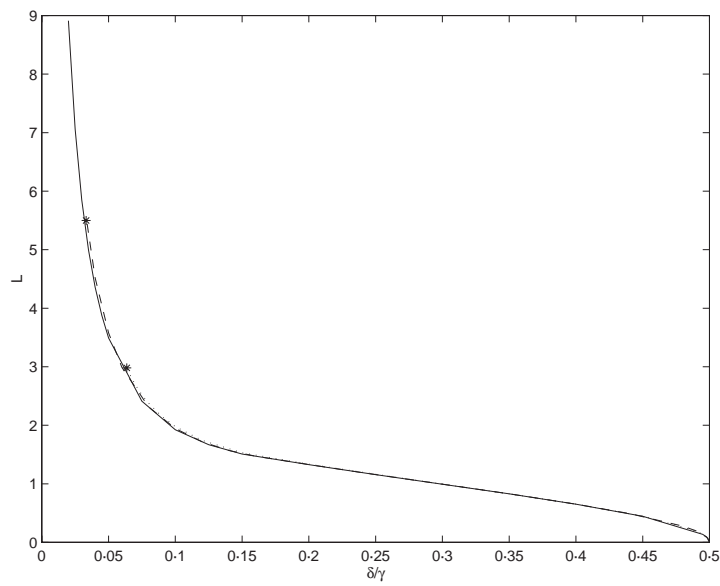
6. Conclusions

In this paper we have used the theory of mixtures to develop a two-phase model of an avascular tumour. The tumour was viewed as a saturated porous medium in which the cells constituted the solid skeleton and were modelled as an ensemble of deformable balloons that interact with each other and the organic liquid in which they are bathed. This liquid contained diffusible nutrients and growth factors which are vital to the tumour's growth and survival. Mass and momentum balance equations were used to derive the governing equations and a key feature of the model was the inclusion of mass exchange between the solid and liquid phases, net expansion of the solid phase indicating growth of the tumour colony.

The governing equations were supplemented by constitutive laws that enable the internal stresses and, in particular, the stress at the interface between the tumour and its surroundings to be calculated. As a result, in addition to investigating the sensitivity of the tumour's equilibrium size and composition to the kinetic cellular parameters, we were also able to study the way in which externally imposed stresses influence tumour growth and to investigate the impact of making cell proliferation depend on cellular stress. As the results of Fig. 9 indicate, the tumour's size decreases as the external loading increases. Referring to Fig. 8, we predict that as the inhibitory influence of mechanical stress on mitosis increases (or, equivalently, the stimulatory influence of mechanical stress on apoptosis increases),



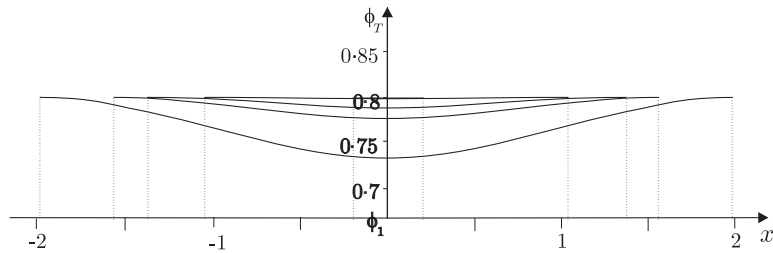
(a)



(b)

FIG. 6. Diagram showing how L depends on $\tilde{\delta}$ when $\tilde{\sigma} = 0$ and $\tilde{\gamma} = 0.002$ (solid line), $\tilde{\gamma} = 0.005$ (dashed line), and $\tilde{\gamma} = 0.01$ (dotted line).

the tumour's equilibrium size decreases. If the inhibitory influence is sufficiently strong the tumour may be eliminated.



x

FIG. 7. Diagram showing how the steady-state tumour size and cell distribution depend on $\tilde{\sigma}$. The vertical dotted lines mark the extent of the tumour. As $\tilde{\sigma}$ increases the equilibrium tumours become smaller and the cell distribution more uniform across the domain. Parameter values: $\tilde{\delta} = 0.001$, $\tilde{\gamma} = 0.01$, $\tilde{\sigma} = 0, 1, 2, 4, 8$.

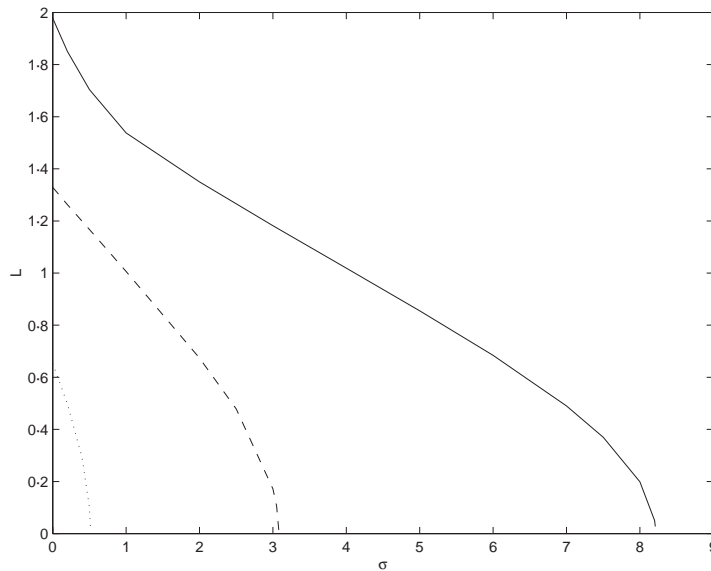


FIG. 8. Diagram showing how the equilibrium size of the tumour L depends on $\tilde{\sigma}$ when $\tilde{\gamma}/\tilde{\delta} = 2.5$ (dotted line), $\tilde{\gamma}/\tilde{\delta} = 5.0$ (dashed line), and $\tilde{\gamma}/\tilde{\delta} = 10.0$ (solid line).

To place these results in context, consider a tumour which is expanding into an organic tissue whose compression generates a stress on the tumour boundary. Our model suggests that, in addition to tumour growth being limited by nutrient availability, the stress from the surrounding tissue, coupled with the stress-dependent reduction in cell proliferation, may limit its growth and equilibrium size. In particular, cell sensitivity to mechanical cues may generate tumour regression or extinction. Equally, as the tumour expands the surrounding tissue may also remodel itself in response to the increasing compressive force that it experiences. This response may lead to overexpression of extracellular matrix (in an attempt to localize the tumour) or degradation of the tissue (in an attempt to relieve the stress the tissue is experiencing).

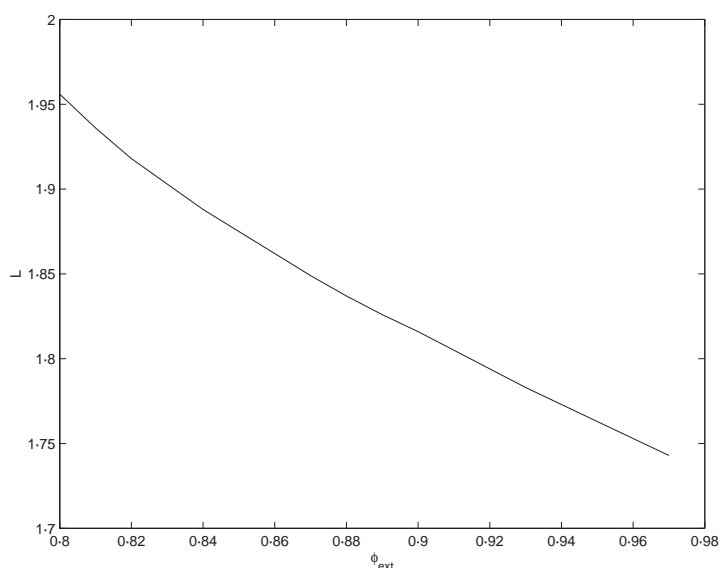


FIG. 9. Diagram showing how the equilibrium size of the tumour L depends on the volume ratio at the boundary. Parameter values: $\tilde{\gamma} = 0.01$, $\tilde{\delta} = 0.001$, and $\tilde{\sigma} = 0$.

In order to validate these predictions, experiments could be performed in which avascular tumours are grown in mechanically stressed environments. This could be achieved by culturing cells in uniform gels of varying stiffness (Helmlinger *et al.*, 1997) or within elastic membranes of varying compliance (the latter experiment resembles ductal carcinoma *in situ*, where the growth of small avascular tumours are confined within the membranes of the breast ducts). Preliminary theoretical work which addresses these issues is contained in Chen *et al.* (2001) and Franks *et al.* (in press). In Chen *et al.* (2001) the restraining force exerted by a poroelastic tissue on a growing tumour is examined while in Franks *et al.* (in press) the growth of an avascular tumour confined by a compliant, cylindrical membrane is studied.

Studying the mechanics of tumour growth raises a number of issues which have long been studied in biomechanics for organic tissues, such as bone, but have not been addressed for solid tumours. These issues include describing the stress–strain relation of the cellular and liquid phases, determining appropriate constitutive laws, measuring the influence of stress on growth and developing a mechanical model for a continuum which grows, lives and dies. Whilst many of these issues remain open problems, we believe that the model presented in this paper represents a step towards their resolution.

In addition to the open questions, there are several relatively straightforward model extensions that merit investigation. These involve specializing the diffusion, growth and absorption terms to render the model more physically realistic and could include the following:

- Allow the diffusion of nutrients and chemical factors to depend on the volume ratio;
- Suppose that the absorption of nutrients is nonlinear;

- Allow the rate of cell proliferation to depend on local levels of extracellular water (water is a basic constituent of cytoplasm); so that if there is no water available then no cell proliferation will occur;
- Allow the rate of apoptosis to depend on cellular stress;
- Consider more complex dependence of the cell proliferation rate on the cellular stress, for example, moderate stresses may promote cell division whereas low and high stresses downregulate cell proliferation and promote cell death. (Similar phenomena occur in bone and muscle, where moderate levels of exercise lead to muscle and bone growth, excessive levels cause damage and insufficient levels cause muscle wastage.)

A second class of model extensions involves introducing additional phases and considering more complex mechanical interactions. For example, in this paper we have assumed, for simplicity, that all tumour cells are identical and that the solid phase is a homogeneous material. In practice, a tumour may contain several functionally disparate clones of tumour cells which differ in their genetic status (for example, cells with normal and abnormal expression of the tumour suppressor gene, p53 and hormone-sensitive and -insensitive cells). Further, *in vivo*, and, to a lesser extent, *in vitro* the cells are contained within an extracellular matrix which may contain other cells such as macrophages, T-cells and fibroblasts. The modelling framework that we have developed generalizes naturally to describe such situations. This paper represents a first step towards our ultimate goal of developing a multicomponent model of a solid tumour.

Acknowledgements

The authors gratefully acknowledge financial support from the following sources: the European Community, through a Research Training Network Project ('Using Mathematical Modelling and Computer Simulation to Improve Cancer Treatment'); the Italian Ministry of University and Scientific and Technological Research; and the Engineering and Physical Sciences Research Council through an Advanced Research Fellowship (HMB).

REFERENCES

- ADAM, J. A. (1987) A mathematical model of tumour growth. II. Effects of geometry and spatial uniformity on stability. *Math. Biosci.*, **86**, 183–211.
- AMBROSI, D. & PREZIOSI, L. (2002) On the closure of mass balance models of tumour growth. *Math: Mod. Meth. Appl. Sci.*, **12**, 737–754.
- BARKER, M. K. & SEEDHOM, B. B. (1997) Articular cartilage deformation under physiological cycling loading. *J. Biomech.*, **30**, 377–381.
- BELLOMO, N. & PREZIOSI, L. (1995) *Modelling, Mathematical Methods and Scientific Computation*. Boca Raton, FL: CRC Press.
- BOWEN, R. M. (1976) Theory of mixtures. *Continuum Physics*. (A. C. Eringen, ed.). New York: Academic.
- BOWEN, R. M. (1980) Incompressible porous media model by use of the theory of mixtures. *Int. J. Eng. Sci.*, **18**, 1129–1148.
- BREWARD, C. J. W., BYRNE, H. M. & LEWIS, C. E. (2002) The role of cell–cell interactions in a two-phase of solid tumour growth. *J. Math. Biol.*, **45**, 125–152.

- BYRNE, H. M. & CHAPLAIN, M. A. J. (1997) Free boundary value problem associated with the growth and development of multicellular spheroids. *Eur. J. Appl. Math.*, **8**, 639–658.
- BYRNE, H. M. (2003) Modelling avascular tumour growth. *Cancer Modelling and Simulation*, Mathematical Biology and Medicine Series, 3. (L. Preziosi, ed.). London: Chapman and Hall/CRC, pp. 75–120.
- BYRNE, H. M., KING, J. R., MCELWAIN, D. L. S. & PREZIOSI, L. (2003) A two-phase model of solid tumour growth. *Appl. Math. Lett.*, **16**, 567–573.
- CARMELIET, P. & JAIN, R. K. (2000) Angiogenesis in cancer and other diseases. *Nature*, **407**, 249–257.
- CHEN, C. Y., BYRNE, H. M. & KING, J. R. (2001) The influence of growth-induced stress from the surrounding medium on the development of multicell spheroids. *J. Math. Biol.*, **43**, 191–220.
- CRAFT, P. S. & HARRIS, A. L. (1994) Clinical prognostic-significance of tumour angiogenesis. *Ann. Oncol.*, **5**, 305–311.
- CURTIS, A. S. G. & SEEHAR, G. M. (1971) The control of cell division by tension or diffusion. *Nature*, **274**, 52–53.
- DREW, D. A. & SEGEL, L. A. (1971) Averaged equations for two-phase flows. *Stud. Appl. Math.*, **50**, 205–231.
- EHLERS, W. (1993) Constitutive equations for granular materials in geomechanical context. *Environmental Sciences and Geophysics*, CISM Courses and Lectures, 337. (K. Hutter, ed.). Berlin: Springer.
- ELLIOTT, C. M. (1985) The Stefan problem with a non-monotone constitutive relation. *IMA J. Appl. Math.*, **35**, 257–264.
- FARINA, A. & PREZIOSI, L. (2000) Deformable porous media and composites manufacturing. *Heterogeneous Media: Micromechanics, Modelling, Methods and Simulations*. (K. Markov & L. Preziosi, eds). Basel: Birkhäuser.
- FARINA, A. & PREZIOSI, L. (2001) On Darcy's law for growing porous media. *Int. J. Nonlinear Mech.*, **37**, 485–491.
- FOLKMAN, J. (1974) Tumor angiogenesis. *Adv. Cancer Res.*, **19**, 331–358.
- FOLKMAN, J. & HOCHBERG, M. (1973) Self-regulation of growth in three dimensions. *J. Exp. Med.*, **138**, 745–753.
- FOWLER, A. C. (1997) *Mathematical Models in the Applied Sciences*. Cambridge: Cambridge University Press.
- FRIJNS, A. J. H., HUYGHE, J. M. & JANSSEN, J. D. (1997) A validation of the quadriphasic mixture theory for intervertebral disc tissue. *Int. J. Eng. Sci.*, **35**, 1419–1429.
- FRANKS, S. J., BYRNE, H. M., UNDERWOOD, J. C. E. & LEWIS, C. E. (in press) Mathematical modelling of comedo ductal carcinoma *in situ* of the breast. *IMAMMB*.
- GATENBY, R. A. & GAWLINSKI, E. T. (1996) A reaction–diffusion model of cancer invasion. *Cancer Res.*, **56**, 5745–5753.
- GREENSPAN, H. P. (1972) Models for the growth of a solid tumour by diffusion. *Stud. Appl. Math.*, **52**, 317–340.
- GREENSPAN, H. P. (1976) On the growth and stability of cell cultures and solid tumours. *J. Theor. Biol.*, **56**, 229–242.
- HEMLINGER, G., NETTI, P. A., LICHTENBELD, H. C., MELDER, R. J. & JAIN, R. K. (1997) Solid stress inhibits the growth of multicellular tumour spheroids. *Nature Biotech.*, **15**, 778–783.
- HOU, J. S., HOLMES, M. H., LAI, W. M. & MOW, V. C. (1989) Boundary conditions at the cartilage-synovial fluid interface for joint lubrication and theoretical verifications. *J. Biomech. Eng.*, **111**, 78–87.
- KUNZ-SCHUGHART, L., DOETSCH, J., MUELLER-KLIESER, W. & GROEBE, K. (2000)

- Proliferative activity and tumourigenic conversion: impact on cellular metabolism in 3-D culture. *Amer. J. Physiol. Cell Physiol.*, **278**, C765–C780.
- LAI-FOOK, S. J. (1988) Pressure–flow behaviour of pulmonary interstitium. *J. Appl. Physiol.*, **64**, 2372–2380.
- LANDMAN, K. & PLEASE, C. P. (2001) Tumor dynamics and necrosis: Surface tension and stability. *IMA J. Maths. Appl. Med. Biol.*, **18**, 131–158.
- MCCELWAIN, D. L. S. & MORRIS, L. E. (1978) Apoptosis as a volume loss mechanism in mathematical models of solid tumour growth. *Math. Biosci.*, **39**, 147–157.
- MOW, V. C. & LAI, W. M. (1979) Mechanics of animal joints. *Ann. Rev. Fluid Mech.*, **11**, 247–288.
- NETTI, P. A., BAXTER, L. T., BOUCHER, Y., SKALAK, R. & JAIN, R. K. (1997) Macro- and microscopic fluid transport in living tissues: Application to solid tumours. *AIChE J.*, **43**, 818–834.
- NICHOLSON, C. (1985) Diffusion from an injected volume of a substance in brain tissues with arbitrary volume fraction and tortuosity. *Brain Res.*, **333**, 325–329.
- PLEASE, C. P., PETTET, G. & MCELWAIN, D. L. S. (1998) A new approach to modelling the formation of necrotic regions in tumours. *Appl. Math. Lett.*, **11**, 89–94.
- PREZIOSI, L. (1996) The theory of deformable porous media and its application to composite material manufacturing. *Surv. Math. Industr.*, **6**, 167–214.
- RAJAGOPAL, K. R. & TAO, L. (1995) *Mechanics of Mixtures*. Singapore: World Scientific.
- SHERRATT, J. A. & NOWAK, M. A. (1992) Oncogenes, anti-oncogenes and the immune response to cancer. *Proc. R. Soc. B*, **248**, 261–271.
- SOREK, S. & SIDEMAN, S. (1986) A porous medium approach for modelling heart mechanics: Part 1. Theory. *Math. Biosci.*, **81**, 1–14.
- STETLER-STEVENSON, W. G., AZNAVOORIAN, S. & LIOTTA, L. A. (1993) Tumor cell interactions with the extracellular matrix during invasion and metastasis. *Ann. Rev. Cell Biol.*, **9**, 541–573.
- SUTHERLAND, R. M. (1988) Cell and environment interactions in tumour microregions: the multicell spheroid model. *Science*, **240**, 177–184.
- SUTHERLAND, R. M. & DURAND, R. E. (1984) Growth of cellular characteristics of multicell spheroids. *Recent Results in Cancer Research*, Vol. 95. Berlin: Springer, pp. 24–49.
- WANG, C. C. (1969) On representations for isotropic functions. II. Isotropic functions of skew-symmetric tensors, symmetric tensors, and vectors. *Arch. Ration. Mech. Anal.*, **33**, 268–287.
- WANG, C. C. (1970) A new representation theorem for isotropic functions: An answer to Professor G. F. Smith's criticism of my papers on representations for isotropic functions. II. Vector-valued isotropic functions, symmetric ten tensor-valued isotropic functions, and skew-symmetric tensor-valued isotropic functions. *Arch. Ration. Mech. Anal.*, **36**, 198–223.
- WARD, J. P. & KING, J. R. (1997) Mathematical modelling of avascular-tumour growth. *IMA J. Math. Appl. Med. Biol.*, **14**, 39–69.
- WARD, J. P. & KING, J. R. (1998) Mathematical modelling of avascular-tumour growth II: Modeling growth saturation. *IMA J. Math. Appl. Med. Biol.*, **15**, 1–42.
- WARD, J. P. & KING, J. R. (1999) Mathematical modelling of the effects of mitotic inhibitors on avascular tumour growth. *J. Theor. Med.*, **1**, 171–211.
- WITELSKI, T. P. (1995) Shocks in nonlinear diffusion. *Appl. Math. Lett.*, **8**, 27–32.
- WU, J. Z. & EPSTEIN, M. (1997) An improved solution for the contact of two biphasic cartilages layers. *J. Biomech.*, **30**, 371–375.
- YANG, M., TABER, L. A. & CLARK, E. B. (1994) A non-linear poroelasticity model for the trabecular embryonic heart. *J. Biomech. Engng*, **116**, 213–223.